

La-doped $\text{Hf}_{0.5}\text{Zr}_{0.5}\text{O}_2$ thin films for high-efficiency electrostatic supercapacitors

Maxim G. Kozodaev, Anna G. Chernikova, Roman R. Khakimov, Min Hyuk Park, Andrey M. Markeev, and Cheol Seong Hwang

Citation: *Appl. Phys. Lett.* **113**, 123902 (2018); doi: 10.1063/1.5045288

View online: <https://doi.org/10.1063/1.5045288>

View Table of Contents: <http://aip.scitation.org/toc/apl/113/12>

Published by the American Institute of Physics

AIP | Conference Proceedings

Get **30% off** all
print proceedings!

Enter Promotion Code **PDF30** at checkout



La-doped $\text{Hf}_{0.5}\text{Zr}_{0.5}\text{O}_2$ thin films for high-efficiency electrostatic supercapacitors

Maxim G. Kozodaev,¹ Anna G. Chernikova,¹ Roman R. Khakimov,¹ Min Hyuk Park,^{2,3} Andrey M. Markeev,^{1,a)} and Cheol Seong Hwang⁴

¹Moscow Institute of Physics and Technology, Institutskii per. 9, 141701 Dolgoprudny, Moscow Region, Russia

²School of Materials Science and Engineering, College of Engineering, Pusan National University, 2, Busandaehak-ro 63beon-gil, Geumjeong-gu, Busan 46241, South Korea

³NaMLab gGmbH/TU Dresden, Noethnitzer Strasse 64, 01187 Dresden, Germany

⁴Department of Materials Science and Engineering and Inter-University Semiconductor Research Center, Seoul National University, Seoul 08826, South Korea

(Received 19 June 2018; accepted 31 August 2018; published online 18 September 2018)

The influence of La content on the ferroelectric properties of $\text{HfO}_2\text{-ZrO}_2$ thin films was examined for integrated electrostatic supercapacitor applications. A transition from ferroelectric to antiferroelectric-like behavior, accompanied by a significant increase of energy storage density value and efficiency, was observed with the increasing La concentration in La-doped $\text{HfO}_2\text{-ZrO}_2$ -based capacitor structures, where the processing temperature remained below 400 °C. The combination of high energy storage density value ($\approx 50 \text{ J/cm}^3$) with high efficiency (70%) was obtained for the film with the highest La content (2.0 mol. %). The 2.0 mol. % La-doped $\text{HfO}_2\text{-ZrO}_2$ -based capacitor structures were field cycled up to 10^9 times and were found to provide $>40 \text{ J/cm}^3$ energy storage density along with up to 80% efficiency. Moreover, the high thermal stability of such capacitors was confirmed. The founded property combination makes the La-doped $\text{HfO}_2\text{-ZrO}_2$ thin films suitable for integrated energy storage and pulse-power devices. *Published by AIP Publishing.*

<https://doi.org/10.1063/1.5045288>

High power electrical energy storage systems, including electrochemical and electrostatic capacitors (ESCs), are becoming critical devices for advanced energy storage technology.^{1,2} Despite the relatively lower energy storage per unit mass compared with the electrochemical devices, the achievable power density of the ESC is generally 3–5 orders of magnitude higher than that of the others, which makes them more preferable for applications that require high power delivery.³ The insufficient total energy storage capacity of ESCs can be significantly improved by utilization of three-dimensional (3-D) nanostructures such as silicon trenches or self-rolling metallic tubes.⁴ These three-dimensional structures require the atomic layer deposition (ALD) technique utilization, because conformal and uniform growth on the high aspect ratio substrates is required. As for the charge storage dielectric layer, aluminum oxide (Al_2O_3) has been the most prominent functional dielectric material for ESC due to its large band gap ($\sim 8.8 \text{ eV}$ for the crystalline α -phase and $\sim 6.7 \text{ eV}$ for the amorphous material), a rather high k -value ($\sim 8\text{--}9$), and highly matured ALD processes. The breakdown field of the Al_2O_3 could be as high as 13.8 MV/cm ,⁵ which can result in the induced polarization of $\approx 11 \mu\text{C/cm}^2$ at the maximum field. As a result, its theoretical energy storage density (ESD) value could be as high as 76 J/cm^3 . However, in practice, the reachable ESD is limited to $\approx 20 \text{ J/cm}^3$ due to the increased leakages and accompanying reliability issues.^{4,6} As a result, it is necessary to introduce new dielectric materials to replace Al_2O_3 for further improvement of ESD.

For such purpose, thin films of higher- k dielectrics, such as HfO_2 or ZrO_2 , which have been already implemented in the mass production of microelectronic devices, are materials of choice.⁷ Recently, pronounced ferroelectric (FE) and antiferroelectric (AFE)-like behavior were discovered both in doped HfO_2 -films,^{8–14} $\text{HfO}_2\text{-ZrO}_2$ (HZO) solid solution,^{15–17} and even doped HZO.^{18,19} According to the literature, FE is attributed to the formation of the non-centrosymmetric orthorhombic phase (o-phase, space group $Pca2_1$),⁸ while the origin of AFE-like behavior is an electric field induced reversible phase transition between the non-polar tetragonal (t-phase, space group $P4_2/nmc$) and polar o-phase.^{15,20} For the sake of simplicity, the term AFE is used throughout the paper keeping in mind that it represents the field induced phase transition mentioned above. In general, both o- and t-phases are characterized by relatively high k values ($\approx 35\text{--}45$ for the t-phase and $25\text{--}35$ for the o-phase), which are beneficial for the purpose of ESC. However, the hysteretic and nonlinear polarization behaviors both in FE and AFE materials require us to take the “efficiency” into consideration, which is usually determined as the ratio $\text{ESD}/(\text{ESD} + \text{loss})$.¹⁴ High efficiency is highly desirable for the ESC applications. Otherwise, it involves higher energy consumption. As can be readily anticipated, FE films generally demonstrate low ESD and low efficiency due to the presence of remnant polarization, which is accompanied with the high energy loss. In contrast, AFE films have almost zero remnant polarization and narrow hysteresis loop area which encompasses much lower loss and high ESD.¹⁴ Moreover, the large polarization change due to field-induced phase transition results in a significant ESD value increase.

^{a)}Electronic mail: markeev.am@mipt.ru

The total AFE film thickness is crucial for ESC energy storage capacity increase by 3-D structures utilization, mentioned earlier. For such purpose, the conventional perovskite-structured AFE films may not be suitable due to their large required thickness to show a robust antiferroelectricity. In the case of the AFE-HfO₂ films, the optimum thickness is usually ~ 10 nm, which is one or two orders of magnitude smaller than perovskite-based AFE materials. Therefore, ALD, in conjunction with the appropriate material choice, is the key enabler for this application of AFE HfO₂-ZrO₂ materials.

Park *et al.* recently reported that 9.2 nm-thick Zr-rich HZO films demonstrated ESD value as high as 45 J/cm^3 at 4.35 MV/cm with an efficiency of $\approx 50\%$.¹⁷ For practical applications, however, in addition to high ESD and efficiency, ESC should exhibit resistance to degradation upon repeated field cycling, i.e., multiple charging/discharging, and reliability at elevated temperatures. In the mentioned work, unfortunately, the ESD value showed a significant reduction to $\approx 30 \text{ J/cm}^3$ at 3.26 MV/cm during the endurance test (up to 10^9 cycles). Hoffmann *et al.* achieved an ESD as high as $\approx 40 \text{ J/cm}^3$ with an efficiency of $\approx 80\%$ at 3.33 MV/cm in a wide temperature range (225–425 K) from the Si-doped (5.6 mol. %) AFE-HfO₂ films.²¹ Ali *et al.* also showed that similar Si-doped (~ 6.0 mol. %) AFE-HfO₂ films could have highly feasible field cycling endurance (up to 10^9 cycles) with an ESD value $\approx 45 \text{ J/cm}^3$ and 60% efficiency.¹⁴ As a further development of such investigations, Lomenzo *et al.* adopted an effective approach of Si/Al-doping to the HZO matrix to improve its energy storage properties.¹⁸ As a result, the AFE Si-doped HZO capacitors exhibited an ESD larger than 30 J/cm^3 with an efficiency of greater than 80% up to 125°C and 10^9 cycles at 4 MV/cm . Recently, a promising ESD of 55 J/cm^3 with an efficiency of $\sim 60\%$ from a carbon-containing HZO film grown at a low ALD temperature (210°C), which could be cycled up to 10^{10} while maintaining an ESD of $\sim 40 \text{ J/cm}^3$, was also reported by Kim *et al.*²² However, film imperfectness in terms of chemical purity, which was shown to be quite important, could be an unreproducible result.

Although the achieved device performances are promising, the high-temperature annealing (500 – 1000°C) required for the film crystallization, especially for the Si-doped HfO₂ (800 – 1000°C),^{14,17,18,21} may impose serious limitations for several cases, where the high-temperature annealing is not allowed. In this aspect, HZO films have shown critical merit over other doped-HfO₂ films as they have a much lower crystallization temperature (400 – 600°C). It has been reported that the Zr-rich HZO (Zr content $\geq 70\%$) films showed AFE-like behavior, whereas the Hf:Zr $\sim 50:50$ showed feasible FE properties. There is an alternative method, however, to induce AFE-like property from the well-established $50:50$ HZO film—the precise La-doping as it was shown previously.¹⁹ Unfortunately, the La content was not varied and such an interesting result was not discussed in detail. However, as we will show in this work, the La:HZO solution could be well crystallized to the o- or t-phase, depending on the La-concentration, even without any post-metallization annealing when the top TiN electrode was grown by a thermal ALD at 400°C . Therefore, this work also reports a detailed characterization of the La:HZO film

with a La-concentration of 2.0 mol. %, which showed highly feasible AFE performance, for its application in ESC devices.

TiN/La:HZO/TiN capacitor structures were formed on silicon wafers with 100 nm-thick plasma-enhanced chemical vapor deposited SiO₂ and 50 nm-thick sputtered W layer for electrical insulation and decreasing the contact resistance, respectively. Both top and bottom TiN electrodes (20 nm-thick) were grown by a conventional thermal ALD method at a substrate temperature of 400°C using TiCl₄ and NH₃ as the Ti-precursor and nitrogen source, respectively. Tetrakis(ethylmethylamino)hafnium (TEMAH), tetrakis(ethylmethylamino)zirconium (TEMAZ), tris(isopropyl-cyclopentadienyl) lanthanum [La(iPrCp)₃], and O₂-plasma were used as the Hf, Zr, La-precursors, and oxygen source, respectively, to grow the 10 -nm-thick La:HZO films at a substrate temperature of 235°C . The La/(Hf + Zr) ALD cycle ratio was varied from $1/32$ to $1/7$ in order to achieve the different La contents (from 0.4 to 2.0 mol. %, respectively). Five different films with 0.4 , 0.7 , 1.0 , 1.4 , and 2.0 mol. % La-concentrations were grown. In addition, a similar HZO-based capacitor structure was also formed as a reference for subsequent experiments. The details for calculation of the La-concentration are presented in the [supplementary material](#). The estimated La content, as well as the Hf/Zr (≈ 1.0) ratio, was confirmed by X-ray photoelectron spectroscopy (XPS) measurements. Top contact pads with area $\approx 2 \times 10^{-5} \text{ cm}^2$ were formed in the top TiN electrode by a lithographic process followed by a plasma-etching in SF₆. No post-metallization annealing was adopted after the top electrode formation. The polarization-electric field (P-E) hysteresis loops were estimated by utilizing a triangular voltage sweeps with 10 kHz frequency. Small-signal capacitance-voltage (C-V) measurements for estimating the dielectric constant value were performed with an AC signal frequency of 10 kHz and 50 mV amplitude.

The structural analysis of the mentioned films was performed by grazing-incidence X-ray diffraction (GIXRD) with Cu K α radiation (the incident angle was set to be 1°). The film surface morphology was studied by scanning electron microscopy (SEM). For this purpose, the top TiN electrode was removed in advance by dipping the sample into H₂O₂ (37%) solution for 15 min at 50°C .

First, the FE/AFE response of La:HZO films in the pristine state, e.g., without any previous field cycling, was analyzed [Fig. 1(a)] in the applied field range $\pm 4.0 \text{ MV/cm}$. The expected FE behavior with the double remnant polarization ($2P_r$) of $\sim 25 \mu\text{C/cm}^2$ could be observed for the undoped HZO film. The smallest La addition (0.4 mol. %) results only in a small coercive field decrease, whereas 0.7 mol. % of La doping led to an increase of $2P_r$ up to $30 \mu\text{C/cm}^2$, which must be related to the increased portion of the o-phase. Further La-addition causes pinching of the hysteresis loop, which finally results in the clear AFE behavior at the highest La-concentration in this work (2.0 mol. %). Such assumption was also confirmed by small-signal C-V measurements which showed the monotonic increase of the dielectric permittivity (k) (see also the [supplementary material](#)) from ~ 30 , which is consistent with the mostly o-phase material, to ~ 45 , which is consistent with the mostly t-phase material

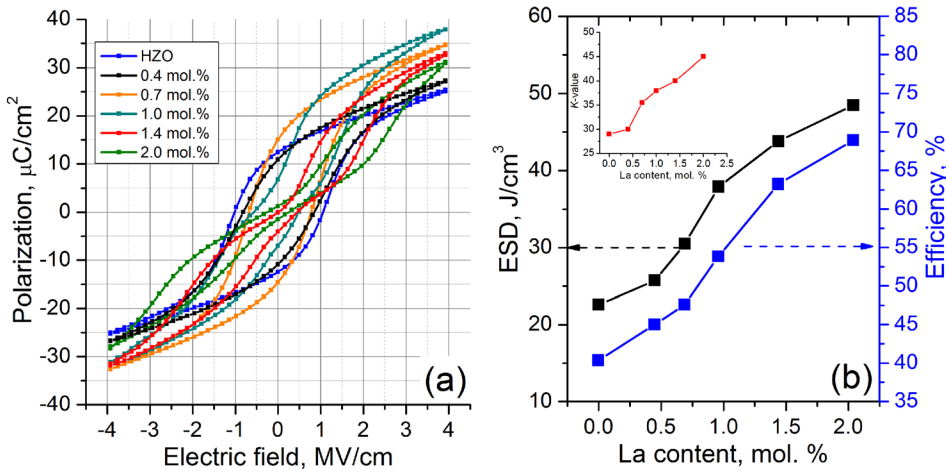


FIG. 1. Influence of La content on the ferroelectric response: P-E curves measured from La:HZO-based capacitors with different La contents at 10 kHz (a); ESD and efficiency as a function of La content (b) [inset: dielectric permittivity (k) as a function of La content].

[inset Fig. 1(b)]. It is worth noticing that the observed rise in k is consistent with almost full suppression of the m-phase formation with the addition of La both in HfO_2 and HZO.^{12,19}

As discussed above, this must be attributed to the preferred t-phase formation, which was also confirmed by XRD, C-V, and SEM measurements (see [supplementary material](#) for the details). As a result, the calculated ESD value significantly increased from 22 J/cm^3 for the pure HZO film up to 49 J/cm^3 for the 2.0 mol. %-doped La:HZO [Fig. 1(b)] with a concurrent increase in the efficiency from $\sim 40\%$ to $\sim 70\%$. The ESD value can also be presented in $\text{Wh} \times \text{kg}^{-1}$ units. The following relation can be written for such conversion:

$$ESD \left[\frac{\text{Wh}}{\text{kg}} \right] = ESD \left[\frac{\text{J}}{\text{cm}^3} \right] \times \frac{0.27}{\rho \left[\frac{\text{g}}{\text{cm}^3} \right]}. \quad (1)$$

Here, ρ denotes the density of the material ($\approx 7.7 \text{ g/cm}^3$ for the $\text{Hf}_{0.5}\text{Zr}_{0.5}\text{O}_2$ solution). Therefore, according to Eq. (1), the ESD value of the 2.0 mol. % La-doped HZO film is $\approx 1.7 \text{ Wh} \times \text{kg}^{-1}$. According to the literature data, the common electrochemical devices possess the ESD value within the range $0.1\text{--}10 \text{ Wh} \times \text{kg}^{-1}$.¹⁴ Therefore, such AFE material utilization already allows reaching the comparable energy storage density. However, the achievable power density of electrochemical devices is only $10^4\text{--}10^6 \text{ W/kg}$ while that one for the proposed ESC can be approximated as $\sim 10^9 \text{ W/kg}$ due to its short discharge time (order of μs).

Therefore, it can be understood that the 2.0 mol. %-doped La:HZO film seemed to be the most promising for energy storage applications, and other performances of this film were further examined below. Further increase in the La

concentration may cause the undesired increase of the crystallization temperature,¹¹ so it was not attempted in this work.

First, the electrochemical impedance spectroscopy (EIS) measurements were carried out, and it was confirmed that the test structure showed a nearly ideal capacitance behavior within the frequency range $10^3\text{--}10^5 \text{ Hz}$ (see [supplementary material](#) for more details). Next, the field-cycling behavior of the optimum AFE film was examined. For this purpose, $\pm 4.0 \text{ MV/cm}$ bipolar pulses with $0.6 \mu\text{s}$ duration were adopted. The evolution of P-E loops with multiple switches and the extracted ESD and efficiency values are presented in Figs. 2(a) and 2(b), respectively. An excellent field-cycling resistance with no hard breakdown up to 10^9 cycles could be achieved even at such high cycling electric field. This remarkable improvement should be attributed to a significant decrease of leakage current with La incorporation into the HZO matrix, reported recently by the authors.

Nonetheless, a notable change in the hysteresis loop shape occurred during cycling as shown in Fig. 2(a), which resulted in a moderate ESD value decrease from 49 J/cm^3 to 40 J/cm^3 . However, the already quite high efficiency (70%) was further increased up to 80% [Fig. 2(b)] due to the decreased hysteresis loop area after the cycling of 10^9 times. Such change in the hysteresis loop shape may be attributed to the charged defects redistribution across the dielectric film, consequent change in the local domain environment, and phase transitions near the AFE/electrode interfaces.^{20,23} Another notable finding from this sample is the following. It has been reported that the pinched hysteresis loop, which is desirable for the ESC application but undesirable for the FE applications, could be induced even in the ferroelectric film

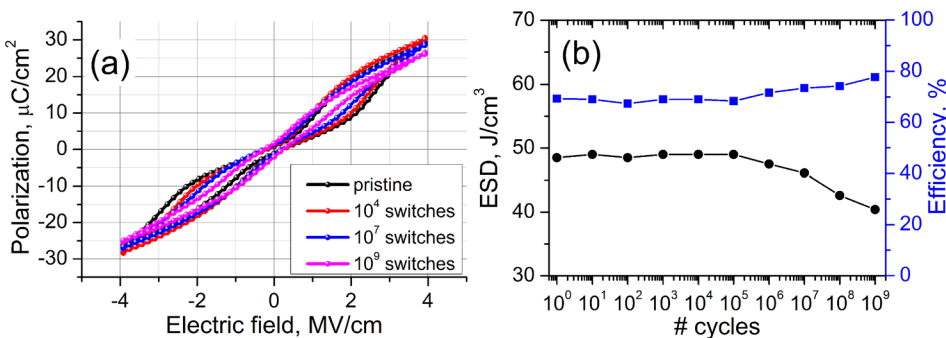


FIG. 2. Room-temperature field-cycling behavior of AFE 2.0 mol. % La:HZO-based ESC: (a) P-E loops, measured after 10^0 (pristine state), 10^4 , 10^7 , and 10^9 switches at $\pm 4.0 \text{ MV/cm}$; (b) ESD and efficiency as a function of cycle number.

due to the pinning of domains by defects.²⁰ Under this circumstance, the pinched loop depinned with the increasing number of cycles, which is highly undesirable for the ESC application. It can be noted that this was not the case in this work; actually, the P-E loop became slimmer as the cycling proceeds revealing the genuine AFE nature of the material.

As it was discussed above, it is necessary that La:HZO-based ESC should be able to operate at elevated temperatures for practical applications. Thus, as the next step, its thermal stability was examined. Figure 3(a) shows the ESD value, loss, and efficiency as functions of temperature for the chosen AFE film. It is clearly seen that both the ESD value and efficiency slight increase from 49 J/cm³ and 70% at 293 K to 55 J/cm³ and 85% at 423 K, respectively, while the energy loss decreases. These observations are consistent with the previous reports for both Zr-rich HZO and AFE Si-doped HfO₂, where the underlying mechanism has been suggested to increase stability or fraction of the non-polar t-phase at elevated temperatures.^{8,15,17,21} Accordingly, the threshold electric field both for $t \rightarrow o$ and $o \rightarrow t$ phase transformations should be higher at elevated temperatures, of which evidence is presented in Fig. 3(b) (both for positive and negative voltages). Here, the threshold field for the two transitions can be extracted from the peak locations on the dP/dE curves, where the peaks at lower and higher absolute E values correspond to the field-induced $o \rightarrow t$ and $t \rightarrow o$ phase transformations, respectively.

The $t \rightarrow o$ phase transition field was ≈ 2.9 MV/cm at 293 K, which increased to ≈ 3.3 MV/cm at 423 K, while the

reverse $o \rightarrow t$ phase transition field also increased from ≈ 1.2 MV/cm to ≈ 1.8 MV/cm, with the same temperature variation. The wide transition temperature range may be attributed to a distribution of Curie temperature of grains with different radii,²¹ but more detailed discussions are beyond the scope of this work. In addition, no degradation of the material was observed during the repeated heating/cooling cycle.

In summary, the ferroelectric—antiferroelectric properties of the La-doped HZO film (Hf/Zr ratio ~ 1) were examined as a function of La concentration up to 2.0 mol. %. All films were not post-metallization annealed but were crystallized mostly to the o-phase and t-phase at low (≤ 1 mol. %) and high (~ 2 mol. %) La-concentrations, respectively, during the top TiN deposition by the thermal ALD method at 400 °C. The film with the highest La-concentration showed typical AFE-like P-E curves, which are highly useful for the electrostatic supercapacitor applications. This film showed a high ESD value (≈ 50 J/cm³) and efficiency (70%) in the pristine state. Such La:HZO film-based ESC demonstrated promising field cycling endurance ($>10^9$ cycles at 4 MV/cm with ESD >40 J/cm³) and thermal stability up to 420 K. The film possessed a genuine AFE nature, so the depinching of the P-E hysteresis loop did not occur during the entire cycling. Rather, the P-E curves became even slimmer after the prolonged cycling, which further enhanced the efficiency up to 80%. Therefore, this material is a highly promising candidate to replace the currently adopted Al₂O₃ film for this type of application.

See [supplementary material](#) for the details of the estimated La content calculation, film characterization, and EIS measurements.

The investigation of energy storage properties as well as the FE/AFE response of multicomponent La:HZO films was supported by the Russian Science Foundation (Project No. 18-19-00527), while the development of fully-ALD grown MIM stacks including ALD TiN electrodes was supported by the Ministry of Education and Science of Russian Federation (Project No. 16.9286.2017/БЧ). The authors also acknowledge the MIPT Shared Facilities Center supported by the Ministry of Education and Science of Russian Federation (Grant No. RFMEFI59417X0014) for access to the equipment.

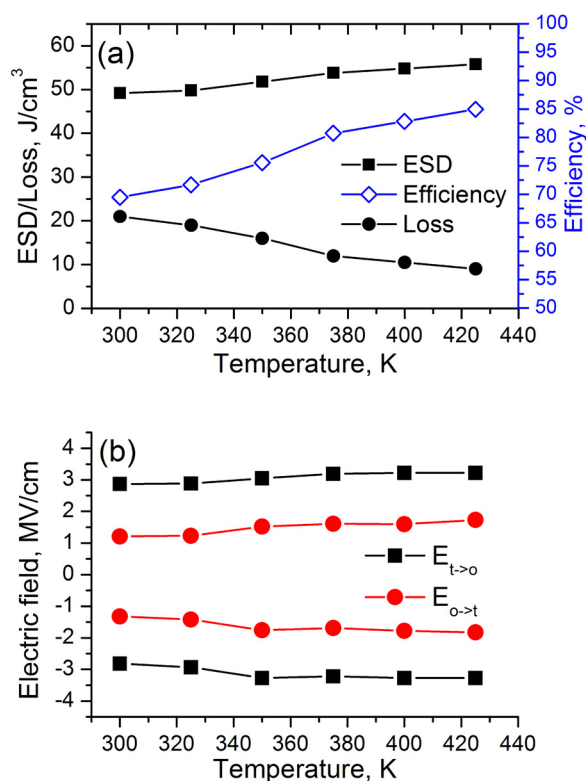


FIG. 3. Energy storage properties of AFE 2.0 mol. % La:HZO-based ESC measured at elevated temperatures in the pristine state: (a) temperature dependent ESD, loss and efficiency values; (b) the threshold fields for $t \rightarrow o$ and $o \rightarrow t$ phase transitions ($E_{t \rightarrow o}$ and $E_{o \rightarrow t}$) measured at various temperatures with the external electric field strength of 4.0 MV/cm.

¹S. A. Sherrill, P. Banerjee, G. W. Rubloff, and S. B. Lee, *Phys. Chem. Chem. Phys.* **13**, 20714 (2011).

²L. C. Haspert, E. Gillette, S. B. Lee, and G. W. Rubloff, *Energy Environ. Sci.* **6**, 2578 (2013).

³K. Yao, S. Chen, M. Rahimabady, M. S. Mirshekarloo, S. Yu, F. E. H. Tay, T. Sriharan, and L. Lu, *IEEE Trans. Ultrason. Ferroelectr. Freq. Control* **58**, 1968 (2011).

⁴R. Sharma, C. C. B. Bufon, D. Grimm, R. Sommer, A. Wollatz, J. Schadowald, D. J. Thurmer, P. F. Siles, M. Bauer, and O. G. Schmidt, *Adv. Energy Mater.* **4**, 1301631 (2014).

⁵J. McPherson, J. Y. Kim, A. Shanware, and H. Mogul, *Appl. Phys. Lett.* **82**, 2121 (2003).

⁶L. C. Haspert, S. B. Lee, and G. W. Rubloff, *ACS Nano* **6**, 3528 (2012).

⁷J. H. Choi, Y. Mao, and J. P. Chang, *Mater. Sci. Eng., R* **72**, 97 (2011).

⁸T. S. Boescke, J. Mueller, D. Brauhaus, U. Schroeder, and U. Boettger, *Appl. Phys. Lett.* **99**, 102903 (2011).

⁹S. Mueller, J. Mueller, A. Singh, S. Riedel, J. Sundqvist, U. Schroeder, and T. Mikolajick, *Adv. Funct. Mater.* **22**, 2412–2417 (2012).

- ¹⁰J. Mueller, U. Schroeder, T. S. Boescke, I. Mueller, U. Boettger, L. Wilde, J. Sundqvist, M. Lemberger, P. Kuecher, T. Mikolajick, and L. Frey, *J. Appl. Phys.* **110**, 114113 (2011).
- ¹¹A. G. Chernikova, D. S. Kuzmichev, D. V. Negrov, M. G. Kozodaev, S. N. Polyakov, and A. M. Markeev, *Appl. Phys. Lett.* **108**, 242905 (2016).
- ¹²M. G. Kozodaev, A. G. Chernikova, E. V. Korostylev, M. H. Park, U. Schroeder, C. S. Hwang, and A. M. Markeev, *Appl. Phys. Lett.* **111**, 132903 (2017).
- ¹³M. Hoffmann, U. Schroeder, T. Schenk, T. Shimizu, H. Funakubo, O. Sakata, D. Pohl, M. Drescher, C. Adelman, R. Materlik, A. Kersch, and T. Mikolajick, *J. Appl. Phys.* **118**, 072006 (2015).
- ¹⁴F. Ali, X. Liu, D. Zhou, X. Yang, J. Xu, T. Schenk, J. Mueller, U. Schroeder, F. Cao, and X. Dong, *J. Appl. Phys.* **122**, 144105 (2017).
- ¹⁵J. Mueller, T. S. Boescke, U. Schroeder, S. Mueller, D. Brauhaus, U. Boettger, L. Frey, and T. Mikolajick, *Nano Lett.* **12**, 4318–4323 (2012).
- ¹⁶M. H. Park, H. J. Kim, Y. J. Kim, W. Lee, T. Moon, and C. S. Hwang, *Appl. Phys. Lett.* **102**, 242905 (2013).
- ¹⁷M. H. Park, H. J. Kim, Y. J. Kim, T. Moon, K. D. Kim, and C. S. Hwang, *Adv. Energy Mater.* **4**, 1400610 (2014).
- ¹⁸P. D. Lomenzo, C.-C. Chung, C. Zhou, J. L. Jones, and T. Nishida, *Appl. Phys. Lett.* **110**, 232904 (2017).
- ¹⁹A. G. Chernikova, M. G. Kozodaev, D. V. Negrov, E. V. Korostylev, M. H. Park, U. Schroeder, C. S. Hwang, and A. M. Markeev, *ACS Appl. Mater. Interfaces* **10**(3), 2701–2708 (2018).
- ²⁰M. Pesic, M. Hoffmann, C. Richter, T. Mikolajick, and U. Schroeder, *Adv. Funct. Mater.* **26**, 7486–7494 (2016).
- ²¹M. Hoffmann, U. Schroeder, C. Kuenneth, A. Kersch, S. Starschich, U. Boettger, and T. Mikolajick, *Nano Energy* **18**, 154–164 (2015).
- ²²K. D. Kim, Y. H. Lee, T. Gwon, Y. J. Kim, H. J. Kim, T. Moon, S. D. Hyun, H. W. Park, M. H. Park, and C. S. Hwang, *Nano Energy* **39**, 390–399 (2017).
- ²³E. D. Grimley, T. Schenk, X. Sang, M. Pesic, U. Schroeder, T. Mikolajick, and J. M. LeBeau, *Adv. Electron. Mater.* **2**, 1600173 (2016).